

# A Study on Thermal Degradation of Organic LEDs Using IR Imaging

G. Nenna,\* G. Flaminio, T. Fasolino, C. Minarini, R. Miscioscia, D. Palumbo, M. Pellegrino

**Summary:** In this paper, we present a correlation study between the working temperature of OLEDs (Organic Light Emitting Diodes) and the electroluminescence and driving voltage changes. The aim is to investigate the relationship between the operating temperature and the aging mechanisms. We have found that performances degradation of devices is strictly related to the glass transition temperature ( $T_g$ ) of organic layers, and that electrical failure is reached only for temperatures higher than  $T_g$ .

**Keywords:** degradation; glass transition; IR imaging; OLED; thermal stress

## Introduction

OLEDs are expected to play a very important role in the market of flat panel displays mainly for their low driving voltage, high brightness and wide angle of view. Since the first efficient OLEDs were successfully fabricated,<sup>[1]</sup> many materials have been developed to improve their performances. A lot of studies on OLED's degradation (aging) have been reported, but to increase devices reliability it is necessary to further investigate these mechanisms. Two main causes have to be considered: the first one is the cathode degradation produced by the moisture<sup>[2–4]</sup> with formation of non-emissive zones, which degrade the optical power efficiency. The other one is the morphological instability of organic layers and can be considered as an "intrinsic degradation": in this case, the electrical stress producing thermal aging is considered.

There are many papers dealing with the thermal aging effects of OLEDs,<sup>[5–7]</sup> which show how an OLED behaves differently during its lifetime for various working regimes at different substrate temperature.<sup>[5]</sup> In

particular, the higher the current density inside the device, the faster the performance degradation because of the current-induced heating (self-heating). To increase the operational stability of OLEDs, several strategies have been developed,<sup>[6,7]</sup> also to study the thermal degradation mechanism, in particular the trend of electroluminescence versus time at different temperatures.<sup>[8]</sup> In this paper, we report a non-invasive method based on IR camera measurements to collect simultaneously light intensity and device's temperature.<sup>[9]</sup>

## Experimental Part

OLEDs under investigation are bottom-emitting with the following structure: glass substrate, a transparent conductor as anode (in our case: Indium doped Tin Oxide, ITO), a Hole Transport Layer (HTL), an Electron Transport Layer (ETL), which is also the emissive layer, and a metallic cathode (we use Aluminium): substrate/ITO/HTL/ETL/Al. In our structure the HTL is N,N'-Bis (3-methylphenyl)-N,N'-diphenylbenzidine (TPD) (20 nm thick) and the ETL is 8-Hydroxyquinoline aluminium (Alq3) (30 nm); ITO-coated glass has been purchased from Delta Technologies and organic materials from Sigma-Aldrich.

ENEA C. R. Portici, v. Vecchio Macello, I-80055 Portici (NA), Italy  
E-mail: giuseppe.nenna@portici.enea.it

Our devices are standard ones, because we are not interested in device performances: indeed our aim is to investigate the aging due to “intrinsic” mechanisms.

Measurements on device stability are generally performed without actively controlling the device temperature and with limited electrical stress.<sup>[1–8]</sup> For our devices, instead, true limits become evident when high voltages and therefore high temperatures are reached.

To analyse the relationships between the various parameters, we made simultaneous current-voltage (I-V), electroluminescence-voltage (EL-V) and temperature-voltage (T-V) measurements, leading the device to electrical, optical and thermal “breakdown” (Figures 1 and 2).

The measurement set-up was:

- an IR (Infrared) camera (AVIO neo-thermo TVS-700), to evaluate the temperature of device,
- a CCD-telescope to collect and send the light to a spectroradiometer (Optronics Laboratories OL770) by an optical fibre,

- a Source-meter (Keithley 2400) to drive the device and to perform the electrical measurements.

The calibration of the IR camera has been performed using a blackbody. We have compared the read temperature for it with the one from the substrate, then we adjusted the response of the camera to obtain the same readings. In this way, we also obtained the emissivity of the substrate,  $\varepsilon$ , found to be about 0.89.

Thermal measurements are made imaging the surface of the glass substrate through which the light emission can be seen. To correctly evaluate the temperature of a working OLED, it is necessary to take into account the difference in temperature between the OLED side of the glass and the mentioned surface. In order to do this, the temperature difference between the two faces has to be previously measured; with an heat fluxmeter, we have heated one face of a bare substrate, measuring the temperature using two thermocouples placed on both sides of the sample. Therefore, the measured temperature on the glass

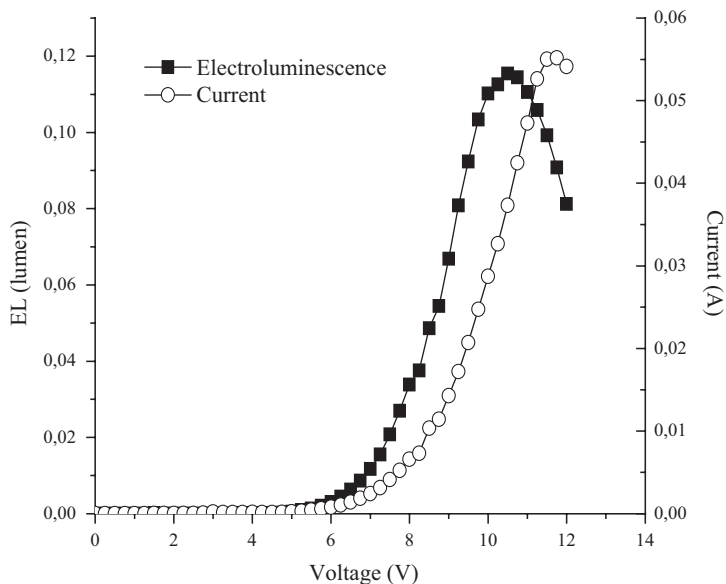


**Figure 1.**

The optical and electrical failures due to the “self-heating” of the device: the reduction of the values after the maxima of the curves shows the device degradation.

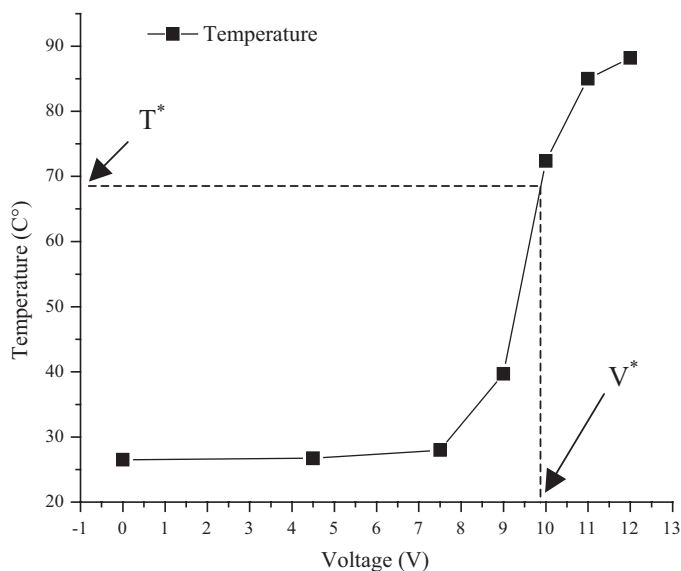


**Figure 2.**

The optical failure, shown in Figure 1, happens when the operating temperature  $T^*$  is at the glass transition temperature of TPD ( $T_g = 68^\circ\text{C}$ ).

can be directly correlated to the temperature of the device.

The measurement of the temperature has to be performed in “stationary” conditions, so we have experimentally determined how long the device power supply has to be held at a fixed voltage to obtain a stable temperature. We call this time “hold time” and it should be long enough to end the thermal transients of the system and short enough to minimise the electrical stress. From experimental data, we have found the optimal hold time to be around 4 seconds. Consequently, each voltage, during a measurement scanning, was maintained for 4 seconds to stabilize the temperature of device without producing a sensible degradation. After this hold time, we acquired the distribution of the temperature on the substrate surface (thermal map) and we tried to relate it to the device’s physical properties (see Fig. 3).

In Figure 3, we can observe that the temperature is higher in the inner part of the device, because the boundaries of its active area exchange heat with the adjacent colder non-active areas. For our purposes, the highest temperature on the surface of

the whole device was considered to get an estimation of the thermally-induced performance decay.

## Results and discussion

Several I-V and EL-V measurements have been made, and always we observed that the optical failure starts before the electrical failure.

As shown in Figure 4, by plotting normalized electroluminescence and current intensity versus voltage in semilog scale, several operating regions can be observed. The “optical failure voltage”  $V^*$  can be defined as the voltage at which the maximum light intensity plateau intersects the polynomial part of the EL curve; in a similar way, the “electrical failure voltage” can be defined using the I-V curve. For the OLED of Fig. 4,  $V^* \approx 9.75\text{ V}$ , 2 V before the electrical failure voltage. From Figure 2, the temperature corresponding to  $V^*$  can be evaluated to be about  $68^\circ\text{C}$ . This temperature falls inside the glass transition temperature range of the TPD.<sup>[6]</sup> In this range of temperatures,

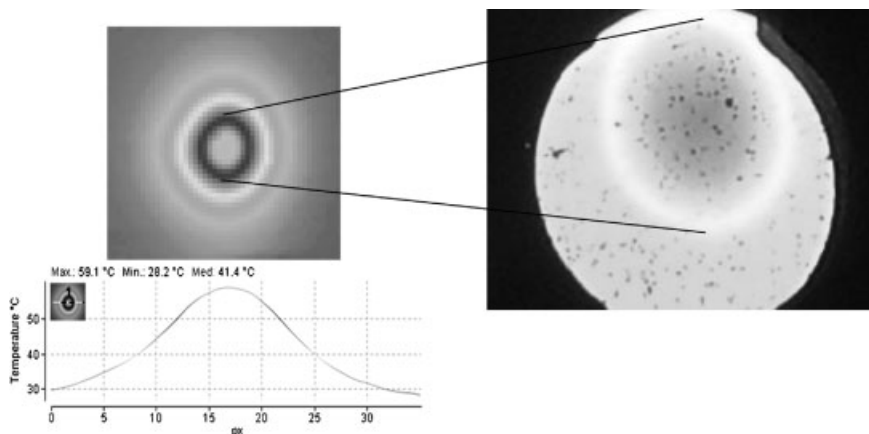


**Figure 3.**

Thermal maps taken from the glass side and temperature profile along a cut-line passing through the centre of the map (px: pixels of the map). Right: Picture of an OLED during operation, showing an evident degradation of electroluminescence. The optical failure starts from the inside of the device.

mechanical, electrical and optical properties of organics show dramatic and rapid changes.<sup>[10]</sup>

We observe that the best candidate as driving force for the aging mechanism is the TPD, because the glass transition temperature of Alq3 is above 150 °C.<sup>[6]</sup>

From the experimental data (see Figure 3), we have observed that highest temperature is not located in the geometrical centre of the device. This fact can be explained considering that the electrical resistivity of ITO ( $4 \cdot 10^{-4} \Omega \cdot \text{cm}$ ) is higher than the resistivity of the Aluminium ( $2 \cdot 10^{-6} \Omega \cdot \text{cm}$ ). Because of this difference, as the distance from power supply contact on ITO anode increases, current density inside the device reduces, so a non-uniformity of the thermal power generation can be observed in the same direction (Fig. 6). In this point of higher temperature, driving the device at voltages approaching  $V^*$ , the electrical stress leads to a local optical failure which can be attributed to a thermally-induced glass transition in the TPD.

Figures 3, 6 and 7 show that the device is brighter at the contours because the boundary effects lead to an accumulation of the current density flow lines. Therefore, if the cause of damage was the current

density, and not the thermal stress, the failure should start from the boundaries of the active area and not from the middle, as instead it happens. As said previously, edges of active zone are cooled by non-active adjacent areas, so their failure is delayed. At high voltages, approaching  $V^*$ , electrical stress produces a significant increase of hole traps near the HTL/ETL interface; they could easily act as recombination centres having a largely non-radiative behaviour,<sup>[12]</sup> and an evident reduction of EL is measured (Figure 1). The electrical stress is correlated to the thermal stress: when the temperature approaches the glass transition range, the induced local film variations act as further non-radiative recombination centres. Therefore, thermal stress leads to the optical failure by the formation of non radiative, but still electrically-active, zones. The electrical damage can be observed in the I–V plot at voltages, greater than the optical failure voltage  $V^*$ , producing a temperature of about 80 °C. Consequently, it can be assumed that the optical failure is due to the glass transition of TPD and not all the physical properties change at the same time and at the same temperature. We can imagine that there are two different “ $T_g$ ”: one for optical and one for electrical parameters. In this way, the

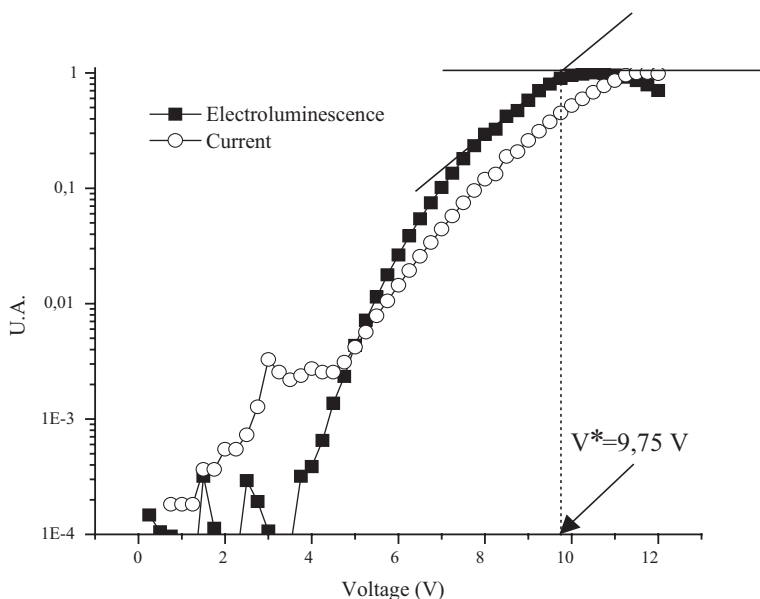


**Figure 4.**

The optical decay region can be defined starting at the intersection of the EL plateau with the adjacent polynomial branch of the curve.

failure temperature higher than  $T_g$  measured by Xiang Zhou et al.<sup>[9]</sup> can be explained.

At the same time, the best configuration stated from Popovic et al., ITO/TPD/NPD/Alq3/Al instead of ITO/NPD/TPD/Alq3/

Al,<sup>[11]</sup> can be explained considering that the TPD layer isn't located at the recombination interface and therefore it harms the device less than in the second configuration. In the ITO/TPD/NPD/Alq3/Al structure, TPD acts only as holes transporter, so its electrical failure dominates and the device can still work at temperatures higher than TPD  $T_g$ , as can be expected according to our results. In the other configuration, the TPD layer is situated on the recombination interface, so its optical failure dominates respect the electrical one.

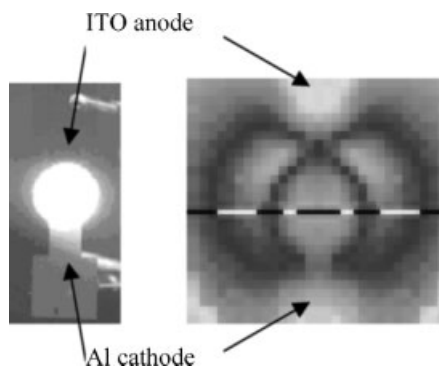


**Figure 5.**

Comparison between a picture of an operating OLED taken from the substrate-side (left) and a thermal map of the same device but from the cathode side (right). In this case, the map is correctly set only for the organics. The higher temperature in proximity of the power supply contact on ITO anode generates the asymmetry bottom-to-up in the thermal map.

#### Optical breakdown estimation

Our set-up allows evaluating the driving voltage producing the optical failure and the corresponding temperature. In general, a T-V curve can be measured.

A device's energy balance can help to estimate the  $I^*$  and  $V^*$  boundaries of the safe operating area. The supplied electrical power ( $W_i$ ) produces two effects: thermal dissipation ( $W_t$ ) and light emission ( $W_o$ ):

$$W_i = W_t + W_o \quad (4)$$

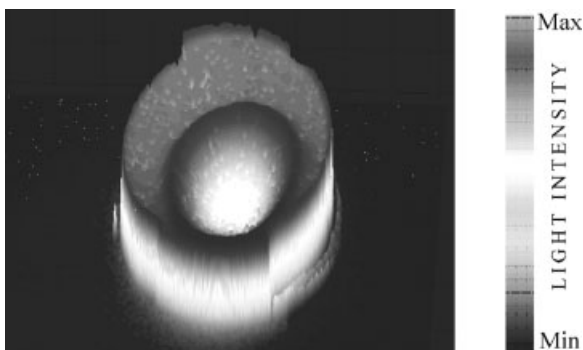


**Figure 6.**

Light intensity shown through 3D elaboration of the same device of Figure 3. In this picture, we can notice the higher intensity of the emission on the boundaries of the active area and the inner “halo” produced by the advance of the morphological changes induced by the thermal stress.

The  $W_t$  term can be expanded to consider the radiative thermal exchange, using the Stefan-Boltzmann law and replace the electrical power  $W_i$  with the  $V \cdot I$  product:

$$VI = \varepsilon\sigma(T^4 - T_0^4)S + f(I) \quad (5)$$

where  $\varepsilon$  is the emissivity,  $\sigma$  is the Stefan-Boltzmann constant,  $V$  is the supplied voltage,  $I$  is the measured current,  $T$  the substrate temperature,  $T_0$  is the starting substrate temperature,  $S$  is the surface of our device and  $f(I)$  is a function that takes into account the other undisclosed terms whose value, for example, can be fitted

from experimental data with a 4-th order polynomial function:

$$f(I) \approx \alpha + \beta \cdot I + \gamma \cdot I^2 + \delta \cdot I^3 + \eta \cdot I^4 \quad (6)$$

For devices having TPD as HTL we have estimated:

$$\alpha = -9.09949E - 6 \text{ [W]}$$

$$\beta = 6.55908 \text{ [WA}^{-1}\text{]}$$

$$\gamma = 244.18584 \text{ [WA}^{-2}\text{]}$$

$$\delta = -6800.56443 \text{ [WA}^{-3}\text{]}$$

$$\eta = 75574.89976 \text{ [WA}^{-4}\text{]}$$

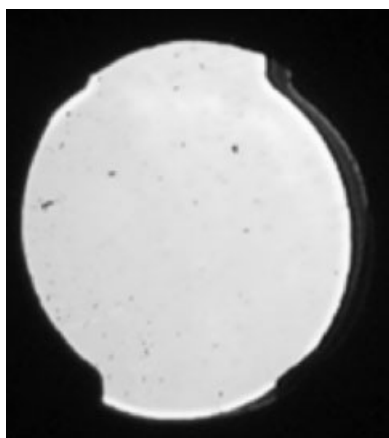


**Figure 7.**

Picture of the same OLED, operated in the safe zone of characteristics.

Therefore, by performing a small amount of measurements in normal operation conditions, we can determine an approximate prediction of device's temperature at a given electrical power and so estimate the maximum safe operating current and voltage without having to drive the OLED to  $V^*$ , i.e. to the  $T_g$  and so irreversibly to its failure. This approach can be applied to electroluminescent organic devices as a non-destructive evaluation of safe operating area.

## Conclusions

In this work, the temperature-dependant electrical properties of organic light-emitting diodes have been studied at different driving

voltages, to better understand their thermal degradation mechanism.

Optical properties show dramatic changes in the glass transition region; instead, electrical failure starts only after the glass transition temperature. Making few measurements, we can predict the evolution of temperature in an OLED as a function of its driving voltage and current. Therefore, given the  $T_g$  of the organic materials, it is possible to estimate the maximum “safe” operating voltage ( $V^*$ ). Otherwise, if  $T_g$  is not known, it can be evaluated using the described experimental set-up driving the device up to its optical failure.

**Acknowledgements:** We would like to thank Dr. Paolo Tassini from ENEA FIM-NANO for his help and suggestions in the final revision of this paper.

[1] C.W. Tang, S.A. Van Slyke, *Appl. Phys. Lett.* **1987**, 51, 913.

[2] T. P. Nguyen, P. Jolinat, P. Destruel, R. Clergereaux, J. Farenç, *Thin Solid Films* **1998**, 325, 175.

[3] H. Mu, H. Shen, D. Klotzkin, *Solid State Electronics* **2004**, 48, 2085.

[4] J. Steiger, S. Karg, R. Schmechel, H. von Seggern, *Synthetic Metals* **2001**, 122, 49.

[5] D. H. Chung, S. W. Hur, S. K. Kim, J. U. Lee, C. H. Kim, J. W. Hong, T. W. Kim, *Current Applied Physics* **2004**, 4, 667–670.

[6] D. F. O'Brian, P. E. Burrows, S. R. Forrest, B. E. Koene, D. E. Loy, M. E. Thompson, *Advanced Materials* **1998**, 14, 1108–1112.

[7] G. Vamvounis, H. Aziz, N-X. Hu, Z. D. Popovic, *Synthetic Metals* **2004**, 143, 69–73.

[8] P. N. M. dos Anjos, H. Aziz, N. X. Hu, Z. D. Popovic, *Organic Electronics* **2002**, 3, 9–13.

[9] X. Zhou, J. He, L. S. Liao, M. Lu, X. M. Ding, X. Y. Hou, X. M. Zhang, X. Q. He, S. T. Lee, *Adv. Mater.* **2000**, 12, 265–269.

[10] L. E. Nielsen, *Mechanical properties of polymers and composites*, vol. 1 Marcel Dekker, inc. New York.

[11] Z. D. Popovic, H. Aziz, N-X. Hu, A-M. Hor, G. Xu, *Synthetic Metals* **2000**, 111–112, 229–232.

[12] D. Y. Kondakov, J. R. Sandifer, C. W. Tang, R. H. Young, *J. Appl. Phys.* **2003**, 93, 1108.